Soft Matter

Dynamic Article Links

Cite this: *Soft Matter*, 2012, **8**, 10288

www.rsc.org/softmatter

PAPER

Mechanics of a liquid drop deposited on a solid substrate

Vlado A. Lubarda*[ab]

Received 30th March 2012, Accepted 16th July 2012
DOI: 10.1039/c2sm25740h

New derivations of Young–Laplace's and Young's equations for a liquid drop deposited on a smooth solid substrate are presented, based on an integral form of equilibrium conditions applied to appropriately selected finite portions of the drop. A simple proof for the gravity independence of the contact angle is constructed and compared with a commonly utilized but more involved proof based on the energy minimization. It is demonstrated that the vertical component of the adhesive force along a triple contact line does not depend on the specific weight of the liquid, provided that the line tension along a triple contact is ignored. The uplifting of the surface of the substrate due to vertical force is calculated by using a linear elasticity theory. The resulting singularity in the vertical displacement and the discontinuity in the radial displacement along a triple contact line are eliminated by incorporating in the analysis the effective width of the triple contact region. It is shown that the radial displacement vanishes on the surface of the substrate outside its contact with a deposited drop.

1. Introduction

The study of a drop's spreading over solid substrates is a fundamental problem in the mechanics of wetting.[1–3] Two central results in this field are Young–Laplace's equation, relating the pressure difference across the liquid–vapor interface of a drop to its curvature and surface tension, $\Delta p = 2\sigma_{lv}\kappa$, and Young's equation, relating the contact angle between a drop and a solid substrate to the surface tensions of the problem, $\cos\theta = (\sigma_{sv} - \sigma_{sl})/\sigma_{lv}$. The indices (sv, sl, lv) designate the solid–vapor, solid–liquid, and liquid–vapor interfaces, and σ stands for the surface tension or energy.

Different derivations of Young–Laplace's and Young's equations are possible. The original derivation by Young[4] and Laplace[5] is based on the consideration of the equilibrium of an infinitesimal element of a pressurized thin membrane. Young's derivation of the expression for the contact angle is based on the consideration of the equilibrium of a material element around a triple contact line, which consists of an infinitesimal segment of a liquid–vapor interface and a thin layer from the surface of a solid substrate (Fig. 1a). The equilibrium condition in the horizontal direction then gives $\sigma_{lv}\cos\theta = \sigma_{sv} - \sigma_{sl}$. Although Young did not refer to it, the vertical component of the surface tension $\sigma_{lv}\sin\theta$ is balanced by the reaction force Y exerted along the contact line by the substrate. The existence and the origin of such adhesive force required for the vertical equilibrium has, however, been discussed in the literature,[2,6] sometimes with the opposing views.[7–10]

Furthermore, a significant amount of research has been devoted to the determination of the shape of the deformed surface of a soft substrate, particularly the uplifting of the surface caused by the vertical component of the capillary force.[11–24] Yet, in many treatises of the subject, the vertical force is not shown on the graph and the consideration of the balance of forces in the vertical direction is omitted altogether.[25] This is in contrast with

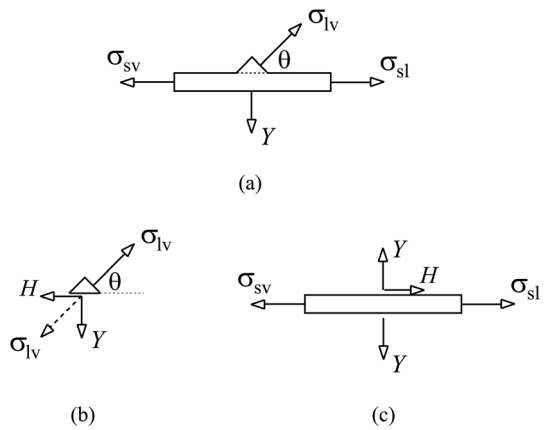

Fig. 1 (a) An infinitesimal element around a triple contact line consisting of a thin surface layer of a solid substrate under surface tensions σ_{sv} and σ_{sl}, and an infinitesimal portion of a liquid–vapor interface under surface tension σ_{lv}. The tangential component $\sigma_{lv}\cos\theta$ is balanced by $\sigma_{sv} - \sigma_{sl}$, and the vertical component $\sigma_{lv}\sin\theta$ by the adhesive force Y. (b) The free-body diagram of the extracted edge ring of the drop which was in contact with the substrate in part (a) along its horizontal side. (c) The free-body diagram of the isolated thin surface layer of the substrate. The free-body diagram from part (a) is recovered by superposing the free-body diagrams from parts (b) and (c).

[a]*Department of Mechanical and Aerospace Engineering, University of California, San Diego, La Jolla, CA 92093-0411, USA. E-mail: vlubarda@ucsd.edu; Fax: +1 858-534-5698; Tel: +1 858-534-3169*
[b]*Montenegrin Academy of Sciences and Arts, Rista Stijovića 5, 81000 Podgorica, Montenegro*

This journal is © The Royal Society of Chemistry 2012

the well-known equilibrium considerations of the floating lenses, or drops deposited on liquid substrates, which are based on Neumann's triangle construction.[26–28]

The variational derivation of Young–Laplace's and Young's equations is based on the energy minimization, in the spirit of the Gibbs thermodynamics.[29] The Young–Laplace's equation follows as the Euler–Lagrange equation of the variational principle, while Young's equation is obtained as the transversality condition accounting for the boundary conditions.[30–35] This approach is particularly appealing because it incorporates in the analysis the gravity, demonstrating explicitly that the specific weight of the liquid does not affect the equilibrium contact angle, provided that the line tension along the triple contact line is omitted from the analysis, which has previously been a topic of an active debate.[36–41]

The variational approach is powerful but mathematically involved, having some physical aspects of the problem embedded in the analysis only implicitly. It is, therefore, desirable to provide a more direct derivation of Young–Laplace's and Young's equations, with an additional insight into the physical origin of the gravity independence of the contact angle. This is accomplished in this paper by using equilibrium conditions from Newtonian mechanics in an integral form, applied to appropriately selected finite portions of the drop, or the entire drop. The presented analysis is remarkably simple and is able to deliver all mechanics results related to the equilibrium drop's shape. As such, it represents a valuable complement to the existing variational analysis, reviewed in the Appendix of this paper. The integral equilibrium conditions furthermore deliver the expressions for the horizontal and vertical components of the adhesive force between a drop and a solid substrate along a triple contact line, demonstrating explicitly their independence from the specific weight of the drop, if the line tension is ignored. In the last section of the paper we shed new light on the determination of the deformed shape of the surface of the substrate by using a linear theory of elasticity, and discuss the singularity of the vertical component and the discontinuity of the radial component of displacement below the triple contact line. The singularities are eliminated by incorporating in the analysis the effective width of the triple contact region. It is shown that the radial displacement vanishes on the surface of the substrate outside its contact with a deposited drop.

2. Derivation of Young–Laplace's equation

Consider the equilibrium configuration of a liquid drop, surrounded by its equilibrium vapor (or another, less dense fluid), deposited on a solid flat substrate (Fig. 2a). The mass density of the liquid is ρ_l, the mass density of the surrounding vapor is ρ_v, and the gravity field is g. Fig. 2b shows a free-body diagram of the portion of the drop above the level $\zeta = z(r)$. The surface tension σ_{lv} acts along the perimeter of radius r at height ζ in the direction tangential to the drop surface. Denoting by $p_l(z)$ and $p_v(z)$ the liquid and vapor pressures at the two sides of the liquid–vapor interface $z = z(\rho)$, where $0 \le \rho \le r$, the hydrostatic equations are

$$p_l(\zeta) = p_l(z) + \gamma_l[z(\rho) - \zeta] \text{ and } p_v(\zeta) = p_v(z) + \gamma_v[z(\rho) - \zeta], \quad (1)$$

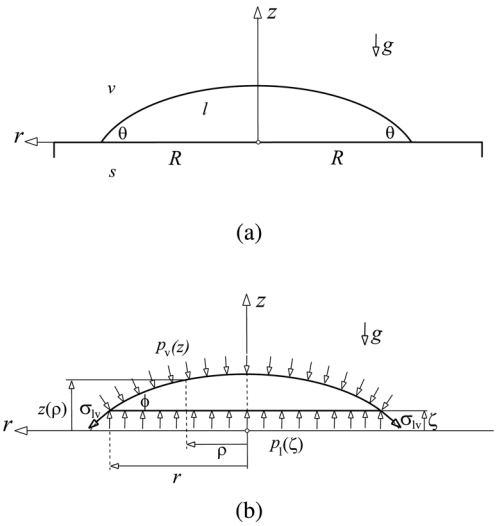

Fig. 2 (a) A liquid drop deposited on a solid substrate in a vapor atmosphere. The gravity field is g, the radius of the contact circle between the drop and the substrate is R, and the contact angle is θ. (b) The free-body diagram of the portion of the drop above the level $\zeta = z(r)$. The liquid pressure at that level is $p_l(\zeta)$. The vapor pressure along the liquid–vapor interface is $p_v(z)$ and the liquid–vapor surface tension along the perimeter of radius r is σ_{lv}.

where $\gamma_l = \rho_l g$ and $\gamma_v = \rho_v g$ are the specific weights of liquid and vapor. In equilibrium the net force should be zero. Thus, making the sum of all force components in the z-direction for the portion of the drop shown in Fig. 2b equal to zero gives

$$\int_0^r \big[p_l(\zeta) - p_v(z)\big] 2\pi\rho \mathrm{d}\rho - 2\pi r\sigma_{lv}\sin\phi - \gamma_l \int_0^r 2\pi\rho[z(\rho) - \zeta]\mathrm{d}\rho = 0. \quad (2)$$

The total force in the z-direction from the pressure p_v, acting over the curved surface of the drop, is equal to the integral of p_v over the projected area orthogonal to the z-direction, which yields the corresponding contribution to the first integral on the left-hand side of eqn (2). The radius of the circular base at the level ζ is r, and ϕ is the indicated angle between the drop's profile $z = z(\rho)$ and the base $z = \zeta$. By using eqn (1), eqn (2) becomes

$$\int_0^r \rho\Delta p\big(z(\rho)\big)\mathrm{d}\rho = \sigma_{lv} r\sin\phi, \quad \Delta p\big(z(\rho)\big) = p_l\big(z(\rho)\big) - p_v\big(z(\rho)\big). \quad (3)$$

The notation $p_l(z(\rho))$ means p_l evaluated at the level $z(\rho)$. The application of the derivative d/dr to both sides of eqn (3) then gives

$$r\Delta p\big(z(r)\big) = \sigma_{lv}\left(\sin\phi + r\cos\phi\frac{\mathrm{d}\phi}{\mathrm{d}r}\right). \quad (4)$$

Since

$$\tan\phi = -\frac{1}{r'}, \quad \sin\phi = \frac{1}{(1+r'^2)^{1/2}}, \quad \cos\phi = -\frac{r'}{(1+r'^2)^{1/2}}, \quad (5)$$

where $r' = \mathrm{d}r/\mathrm{d}\zeta$, and since $\mathrm{d}r'/\mathrm{d}r = r''/r'$, we have

$$\frac{\mathrm{d}\phi}{\mathrm{d}r} = \frac{1}{1+r'^2}\frac{r''}{r'}. \tag{6}$$

The substitution of eqn (6) into eqn (4) yields

$$\Delta p = 2\sigma_{\mathrm{lv}}\kappa, \quad 2\kappa = \frac{1}{r(1+r'^2)^{1/2}} - \frac{r''}{(1+r'^2)^{3/2}}, \tag{7}$$

which is the axisymmetric form of Young–Laplace's equation, expressing the equilibrium of an infinitesimal element of a drop's surface locally. The derivation also delivers the geometric expression for the mean curvature κ in terms of r and its derivatives, as given in eqn (7).

3. Contact angle and its gravity independence

Fig. 3a shows a free-body diagram of one-half of the drop, together with a thin layer of the solid substrate on which it is deposited. The forces with the components in the longitudinal direction are only shown, as only they participate in the equilibrium condition in that direction. For the general use of free-body diagrams in mechanics, ref. 42 and 43 can be consulted. The surface tensions within the solid–liquid and solid–vapor interfaces are denoted by σ_{sl} and σ_{sv}. The surface tension σ_{lv} acts in the horizontal direction along the curved liquid–vapor interface of the vertical cut through the drop surface. The line tension along the triple contact line is denoted by τ, and in the free-body diagram of Fig. 3a it acts at the two points where the vertical cut intersects the triple contact line. The equilibrium condition in the longitudinal direction is obtained by making the sum of all force components in the longitudinal direction, acting on the free-body shown in Fig. 3a, equal to zero. This gives

$$(\sigma_{\mathrm{sl}} - \sigma_{\mathrm{sv}})2R + \sigma_{\mathrm{lv}}L + 2\tau - \int_A \left[p_{\mathrm{l}}(\zeta) - p_{\mathrm{v}}(\zeta)\right]\mathrm{d}A = 0, \tag{8}$$

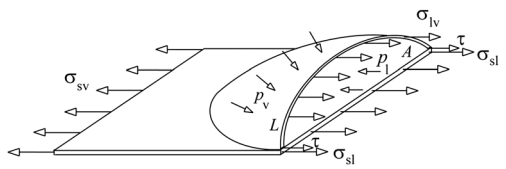

(a)

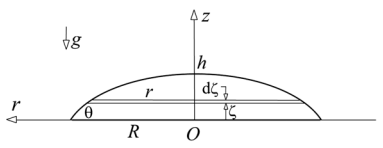

(b)

Fig. 3 (a) The free-body diagram of one-half of the drop atop a thin substrate layer. The forces with the components in the longitudinal direction are only shown. The surface tensions of the solid–liquid, solid–vapor, and liquid–vapor interfaces are σ_{sl}, σ_{sv}, and σ_{lv}. The line tension along the triple contact line is τ. (b) The mid-section of the drop with indicated variables used in the integration procedure.

where L is the length of the liquid–vapor interface in the middle cross-section of the drop, and A is the area of that cross-section. Since liquid pressure is constant along the line ζ = const. (Fig. 3b), the pressure difference $p_{\mathrm{l}}(\zeta) - p_{\mathrm{v}}(\zeta)$ along this line can be calculated as the pressure difference across the liquid–vapor interface at $z = \zeta$, which is given by Young–Laplace's expression eqn (7), $\Delta p = 2\sigma_{\mathrm{lv}}\kappa$. Consequently, by writing $\mathrm{d}A = 2r\mathrm{d}\zeta$, the area integral in eqn (8) becomes

$$\int_A \left[p_{\mathrm{l}}(\zeta) - p_{\mathrm{v}}(\zeta)\right]\mathrm{d}A = 2\sigma_{\mathrm{lv}}\int_0^h (2\kappa r)\mathrm{d}\zeta, \tag{9}$$

with h as the height of the drop. Furthermore, it can be verified from eqn (7) that

$$2\kappa r = (1+r'^2)^{1/2} - \frac{\mathrm{d}}{\mathrm{d}\zeta}\left[\frac{rr'}{(1+r'^2)^{1/2}}\right]. \tag{10}$$

When this is substituted into the integral on the right-hand side of eqn (9), there follows

$$\int_0^h (2\kappa r)\mathrm{d}\zeta = \frac{L}{2} - R\cos\theta, \tag{11}$$

because $(1 + r'^2)^{1/2}\mathrm{d}\zeta = \mathrm{d}L$ is the arc length along the liquid–vapor interface in the (z, r) plane, $r'(h) = 0$ by the symmetry around the z axis, and

$$r'(0) = -\cot\theta, \quad \frac{r'(0)}{\left[1+r'^2(0)\right]^{1/2}} = -\cos\theta. \tag{12}$$

Consequently, eqn (9) gives

$$\int_A \left[p_{\mathrm{l}}(\zeta) - p_{\mathrm{v}}(\zeta)\right]\mathrm{d}A = \sigma_{\mathrm{lv}}(L - 2R\cos\theta). \tag{13}$$

By introducing eqn (13) into eqn (8), we obtain the generalized Young's equation, also referred to as the Boruvka–Neumann equation,[44,45]

$$\sigma_{\mathrm{sl}} - \sigma_{\mathrm{sv}} + \sigma_{\mathrm{lv}}\cos\theta + \frac{\tau}{R} = 0, \tag{14}$$

i.e.,

$$\cos\theta = \frac{\sigma_{\mathrm{sv}} - \sigma_{\mathrm{sl}}}{\sigma_{\mathrm{lv}}} - \frac{\tau}{R\sigma_{\mathrm{lv}}}. \tag{15}$$

If the line tension is ignored, eqn (15) reduces to Young's equation. The presented derivation provides an explicit proof that the contact angle θ between the drop and a substrate is independent of the gravity, or the specific weight of liquid, if the line tension is ignored, and if the surface tension is assumed to be independent of the curvature. An alternative proof available in the literature,[31,33] based on the variational approach and energy minimization, is longer and more mathematically involved (Appendix).

If the line tension is retained in the analysis, the gravity affects the contact angle through the radius R, appearing in the second term on the right-hand side of eqn (15), which depends on the volume and the specific weight of the liquid. Since the typical value of the ratio $\tau/\sigma_{\mathrm{lv}}$ is about 1 nm,[46] and can be either positive or negative,[47] the line tension effect cannot be neglected for

 This journal is © The Royal Society of Chemistry 2012

droplets of initial radius below about 100 nanometers.[48,49] The positive line tension increases the equilibrium value of the contact angle, while the negative line tension decreases it.[45]

4. Vertical component of the adhesive force

Fig. 4 shows a free-body diagram of the equilibrium configuration of the entire liquid drop. The liquid pressure at the solid–liquid interface is p_l^0, and the constant vapor pressure at the solid–vapor interface is p_v^0. Denoting by $p_l(z)$ and $p_v(z)$ the liquid and vapor pressures at the two sides of the liquid–vapor interface, $z = z(r)$, we can write

$$p_l^0 = p_l(z) + \gamma_l z(r) \text{ and } p_v^0 = p_v(z) + \gamma_v z(r). \tag{16}$$

If H and Y are the horizontal and vertical components of the adhesive force along the triple contact line, the equilibrium condition in the vertical direction for the entire drop is

$$\int_0^R \left[p_l{}^0 - p_v(z)\right] 2\pi r \mathrm{d}r - 2\pi R Y - \gamma_l \int_0^R 2\pi r z(r) \mathrm{d}r = 0. \tag{17}$$

Since, from eqn (16),

$$p_l{}^0 - p_v(z) = p_l(z) - p_v(z) + \gamma_l z(r), \tag{18}$$

the substitution of eqn (18) into eqn (17) gives

$$Y = \frac{1}{R}\int_0^R \Delta p r \mathrm{d}r, \quad \Delta p = p_l(z) - p_v(z), \tag{19}$$

i.e.,

$$Y = \frac{\sigma_{lv}}{R}\int_0^R 2\kappa r \mathrm{d}r, \tag{20}$$

because $\Delta p = 2\sigma_{lv}\kappa$ by eqn (7).

Further progress with eqn (20) can be made by observing that

$$2\kappa r \mathrm{d}r = \mathrm{d}\left[\frac{r}{(1+r'^2)^{1/2}}\right]. \tag{21}$$

When this is used to evaluate the integral in eqn (20), there follows

$$\int_0^R 2\kappa r \mathrm{d}r = R\sin\theta, \quad \sin\theta = \frac{1}{\left[1 + r'^2(0)\right]^{1/2}}. \tag{22}$$

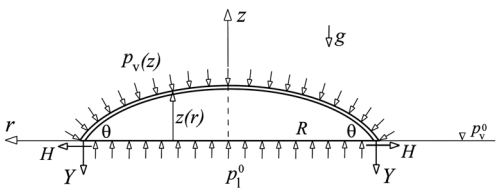

Fig. 4 The free-body diagram of the entire drop. The components of the adhesive force along the triple contact line are H and Y. The liquid pressure at $z = 0$ is $p_l{}^0$, and the vapor pressure over the surface of the drop is $p_v(z)$.

Thus, the adhesive force eqn (20) becomes

$$Y = \sigma_{lv}\sin\theta. \tag{23}$$

In the absence of gravity eqn (17) reads $(p_l - p_v)R^2\pi - 2R\pi Y = 0$. Since $\Delta p = p_l - p_v = 2(\sigma_{lv}/R)\sin\theta$, eqn (23) follows.

5. Horizontal component of the adhesive force

We next elaborate on the expression for the horizontal component of the adhesive force. Fig. 5a shows a free-body diagram of a thin surface layer of the solid substrate, with a removed drop. For the consideration of equilibrium in the horizontal direction, only the forces in the horizontal plane of the substrate are shown. The equilibrium condition in the longitudinal direction is then

$$(\sigma_{sv} - \sigma_{sl})2R - 2RH - 2\tau = 0. \tag{24}$$

The horizontal component of the adhesive force is, therefore,

$$H = \sigma_{sv} - \sigma_{sl} - \frac{\tau}{R}. \tag{25}$$

If the longitudinal equilibrium is imposed to one half of the drop alone (free-body diagram without the solid substrate underneath), as shown in Fig. 5b, the condition for the longitudinal equilibrium is

$$\sigma_{lv}L - 2RH - \int_A \left[p_l(\zeta) - p_v(\zeta)\right]\mathrm{d}A = 0. \tag{26}$$

The integral in eqn (26) is equal to $\sigma_{lv}(L - 2R\cos\theta)$, as shown in Section 3, so that eqn (26) yields an alternative expression for the horizontal component of the adhesive force, which is

$$H = \sigma_{lv}\cos\theta. \tag{27}$$

Furthermore, by reconciling eqn (25) and eqn (27), we recover the modified Young's eqn (15).

6. The shape of the deformed substrate surface

In the absence of line tension τ, the horizontal component of the adhesive force $H = \sigma_{lv}\cos\theta$ is balanced by the surface tension difference $\sigma_{sv} - \sigma_{sl}$, due to wetting of the solid surface below the drop. We assume that this self-equilibrating system of tangential forces within the infinitesimally thin surface layer of the substrate does not induce an appreciable deformation in the bulk of the

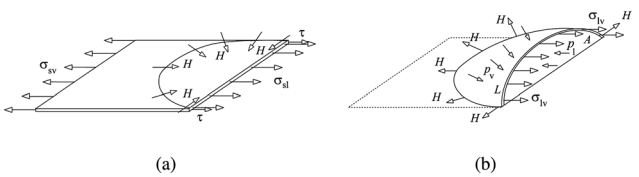

Fig. 5 (a) The free-body diagram of a thin surface layer of the solid substrate, with a removed drop above it. For the consideration of equilibrium in the horizontal direction, only the forces within the plane of the substrate are shown. (b) The free-body diagram of one-half of the drop above the substrate layer from part (a).

substrate beneath it. This is consistent with a common practice of neglecting deformation of a thick substrate due to surface tension along the bounding free surfaces of the substrate. Consequently, we consider the substrate deformation caused by the vertical loading only. If there is no gravity, this loading consists of the uniform vapor pressure p_v^0 all over the substrate, and the self-equilibrated loading shown in Fig. 6, which consists of Laplace's pressure $p = 2\kappa\sigma_{lv}$ and distributed line force $Y = R\kappa\sigma_{lv}$. For a sufficiently stiff substrate, the deformation caused by this loading is negligibly small, but may be more observable or measurable for a softer substrate. The deformed surface shape of such soft substrates will be determined in this section by using the linear elasticity theory. Denoting by $w = w(r)$ the upward displacement of the points on the surface of the substrate, we can write

$$w = w^p + w^Y. \tag{28}$$

The expression for the displacement w^p is well-known from the classical linear elasticity,[50–52] and is given by

$$w^p = -\frac{2(1-\nu)pR}{\pi G}\begin{cases} E\left(\frac{r}{R}\right), & r \le R, \\ \frac{r}{R}\left[E\left(\frac{R}{r}\right) - \left(1-\frac{R^2}{r^2}\right)K\left(\frac{R}{r}\right)\right], & r \ge R, \end{cases} \tag{29}$$

where G and ν are the elastic shear modulus and the Poisson ratio of the substrate material (assumed to be isotropic), and

$$K(k) = \int_0^{\pi/2} \frac{d\psi}{\left(1-k^2\sin^2\psi\right)^{1/2}}, \quad E(k) = \int_0^{\pi/2} \left(1-k^2\sin^2\psi\right)^{1/2} d\psi \tag{30}$$

are the complete elliptic integrals of the first and second kinds, respectively. The surface depression at the center is $-w^p(0) = (1-\nu)pR/G$.

The expression for w^Y can be conveniently obtained by superimposing the solutions of two loadings and by performing an appropriate limit. The two loadings are the pressure p over the circle of radius R, and the tension of magnitude p over the circle of radius $R + \Delta R$ ($\Delta R \ll R$). In the limit, the resulting displacement is

$$w^Y(r) = \frac{dw^p}{dR}\Delta R, \quad p\Delta R \to Y, \tag{31}$$

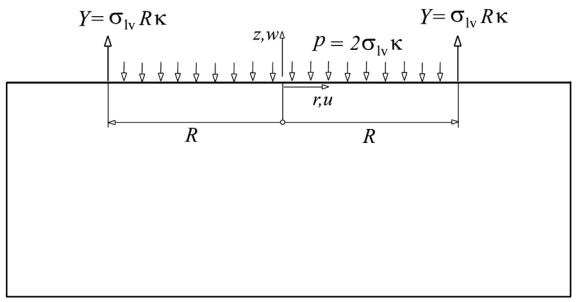

Fig. 6 A self-equilibrated loading on the surface of the substrate, consisting of pressure $p = 2\kappa\sigma_{lv}$ and distributed line force $Y = R\kappa\sigma_{lv}$.

to first order in ΔR. By using eqn (29), and recalling that[53]

$$\frac{dE(k)}{dk} = \frac{1}{k}\left[E(k) - K(k)\right], \quad \frac{dK(k)}{dk} = \frac{1}{k}\left[\frac{E(k)}{1-k^2} - K(k)\right], \tag{32}$$

it follows that

$$w^Y = \frac{2(1-\nu)Y}{\pi G}\begin{cases} K\left(\frac{r}{R}\right), & r \le R, \\ \frac{R}{r}K\left(\frac{R}{r}\right), & r \ge R. \end{cases} \tag{33}$$

The corresponding displacement at the center is $w^Y(0) = (1-\nu)Y/G$. The expression (33) is a novel expression, complementing an earlier representation of w^Y given by (3.96a) of ref. 52, page 77.

Since the line force (per unit length of the triple contact line) is $Y = R\kappa\sigma_{lv} = \sigma_{lv}\sin\theta$, while the pressure $p = 2\kappa\sigma_{lv}$, with $R\kappa = \sin\theta$, the substitution of eqn (29) and eqn (33) into eqn (28) gives the expression for the vertical displacement

$$w = \frac{2w_0}{\pi}\begin{cases} K\left(\frac{r}{R}\right) - 2E\left(\frac{r}{R}\right), & r \le R, \\ \frac{r}{R}\left[\left(2-\frac{R^2}{r^2}\right)K\left(\frac{R}{r}\right) - 2E\left(\frac{R}{r}\right)\right], & r \ge R. \end{cases} \tag{34}$$

In this expression,

$$w_0 = \frac{(1-\nu)\sigma_{lv}}{G}\sin\theta \tag{35}$$

is the magnitude of the displacement at the center, $w_0 = -w(0)$. A simple representation of the expression for the vertical displacement w given by eqn (34) is novel. From eqn (35), we can identify the elasto-capillary length scale $l_0 = (1-\nu)\sigma_{lv}/G$, which represents the ratio of the surface tension σ_{lv} and the elastic parameter $G/(1-\nu)$. For example, for a water drop on a Teflon substrate, $l_0 \approx 1.13$ Å, while for a mercury drop on a Teflon substrate, $l_0 \approx 7.5$ Å. In the calculations, it was taken that the shear modulus and Poisson's ratio of Teflon were $G = 0.35$ GPa and $\nu = 0.46$, respectively. The liquid–air surface tension σ_{lv} of water is taken to be 0.073 N m^{-1} and of mercury 0.486 N m^{-1}.[54] For very deformable (silicon gel type) elastomer substrates, with the shear modulus of 1 MPa and Poisson's ratio close to 0.5, the length l_0 is about 350 Å. For some gels and biological tissues, the shear modulus may be 50 kPa or less, and l_0 can be of the order of micrometers.[11,12,55]

For a given contact angle, determined from Young's equation $\cos\theta = (\sigma_{sv} - \sigma_{sl})/\sigma_{lv}$, and for a given volume of the drop $V_0 = 4\pi R_0^3/3$, the radius R of a spherical cap drop, appearing in eqn (34), is

$$R = \frac{2R_0\cos\frac{\theta}{2}}{\sin^{1/3}\frac{\theta}{2}\left(1+2\cos^2\frac{\theta}{2}\right)^{1/3}}. \tag{36}$$

Fig. 7a shows the plot of a nondimensional displacement profile $w(r)/w_0$. Fig. 8 shows the two displacement contributions w^p and w^Y (normalized by w_0). The linear elasticity predicts a displacement singularity for w^Y, and thus w, along the triple contact line $r = R$. The singularity can be eliminated by introducing a small but finite thickness of the liquid–vapor interface layer and by considering Y to be distributed rather than

 This journal is © The Royal Society of Chemistry 2012

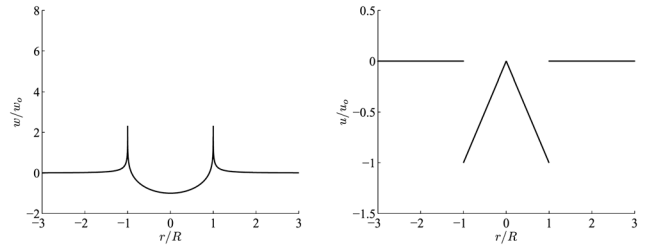

(a) (b)

Fig. 7 (a) The normalized vertical displacement ($w = w^p + w^Y$) of the surface of the substrate due to combined (p, Y) loading shown in Fig. 6. The normalizing displacement factor w_0 is specified by eqn (35). (b) The corresponding normalized radial displacement ($u = u^p + u^Y$). The normalizing displacement factor u_0 is specified by eqn (38).

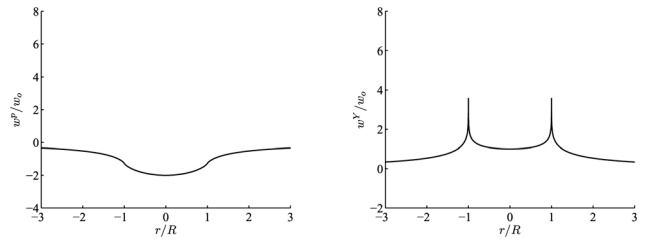

(a) (b)

Fig. 8 The normalized vertical displacement contributions w^p and w^Y from: (a) pressure p, and (b) line loading Y. Their sum gives the displacement profile shown in Fig. 7a. The normalizing displacement factor is specified by eqn (35).

concentrated line force acting on the surface of the substrate. Such an approach, previously used in ref. 11 and 12 will be discussed further is Section 6.2. A nonlinear continuum model may also be used, although an atomistic/molecular dynamics approach is in essence needed to predict the uplifting of the substrate very close to a triple contact line. Analytical and experimental determination of the deformation of a highly elastic silicone gel substrate due to a 10 μL water drop has recently been reported by Jerison *et al.*,[23] who measured surface and bulk deformation of a thin elastic film near a three-phase contact line using fluorescence confocal microscopy, but in their analytical study they assumed that the contact angle is $\theta = \pi/2$. Related work also includes the contributions.[16–24,56–59] Earlier studies considered drops which were deposited on circular plates with the bending stiffness,[13] the analysis based on the plain strain approximation,[55,60] and the analysis of a liquid droplet deposited in the middle of an elastic isotropic thin solid sheet,[15] rather than a semi-infinite substrate as in this paper. The formation of circular ridges by the action of capillary forces can have significant effects on the functioning of MEMS and other micro/nano devices, lubrication of magnetic hard disks, molten solder spreading in electronic packaging, painting, coating, anti-stain or anti-frost treatments, *etc.* For example, the created wetting ridge can significantly increase the spreading time of a deposited drop, or can increase the roughness of the surface of a substrate upon the drop's evaporation, both having important technological consequences.[16]

6.1. Radial displacement

Fig. 7b shows the radial displacement of the points on the surface of the substrate, obtained from

$$u = u_0 \begin{cases} -\dfrac{r}{R} & r < R, \\ 0, & r > R, \end{cases} \tag{37}$$

where

$$u_0 = \frac{(1-2\nu)\sigma_{1v}\sin\theta}{2G}. \tag{38}$$

The expression for the radial displacement eqn (37) is derived by the superposition of two contributions[61]

$$u^p = -\frac{p(1-2\nu)}{4G} \begin{cases} r & r \le R, \\ \dfrac{R^2}{r}, & r \ge R, \end{cases} \tag{39}$$

and

$$u^Y = \frac{Y(1-2\nu)}{2G} \begin{cases} 0 & r < R, \\ \dfrac{R}{r}, & r > R, \end{cases} \tag{40}$$

with $p = 2Y/R$ and $Y = \sigma_{1v}\sin\theta$. The plots of the displacement contributions u^p and u^Y are shown in Fig. 9. The displacement u^p is linear, while $u^Y = 0$ within $r < R$. In addition, $u^p = -u^Y$ for $r > R$, so that $u = 0$ for $r > R$ (Fig. 7b). The negative values of the radial displacement u for $r < R$ mean that the radial displacement there is toward the center. The linear elasticity also predicts that the radial displacement is discontinuous at $r = R$. The radial displacement features shown in Fig. 7b were not previously noted or discussed in the literature. The displacement singularity and the displacement discontinuity will be eliminated in Section 6.2 by distributing Y over a small, but finite thickness. The linear elasticity predictions of infinite vertical displacement and discontinuous radial displacement can be interpreted as the indications of the tendency for large vertical displacement and large gradient of the radial displacement below the triple contact line. If the substrate is incompressible ($\nu = 1/2$), the radial displacement vanishes at all points on the surface of the substrate ($u = u^p = u^Y = 0$).

6.2. Finite thickness of the surface layer

To eliminate the singularity in the vertical displacement and the discontinuity in the radial displacement under the concentrated line force, it is assumed that the line force Y is distributed over a small but finite thickness, related to the thickness of the interface of the liquid–vapor layer and the molecular interactions between the liquid drop and the solid substrate. This thickness may vary from 1 nm for harder substrates to millimicrons for softer rubber or gel substrates.[6,11,12,20] The vertical displacement along the surface of the substrate due to the loading shown in Fig. 10 is readily obtained from eqn (29) by superposing the displacements due to tensile loading of magnitude q along $r \le R$ and the tension loading of magnitude q along $r < R_0$. This gives

$$w^q = \frac{2(1-\nu)qR}{\pi G} W^q, \tag{41}$$

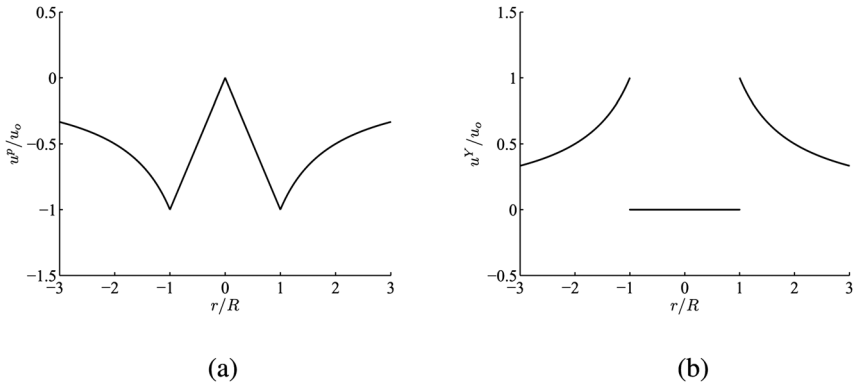

Fig. 9 The normalized radial displacement contributions u^p and u^Y from: (a) pressure p, and (b) line loading Y. Their sum gives the displacement profile shown in Fig. 7b. The normalizing displacement factor is u_0 from eqn (38), with $p = 2Y/R$ and $Y = \sigma_{lv}\sin\theta$.

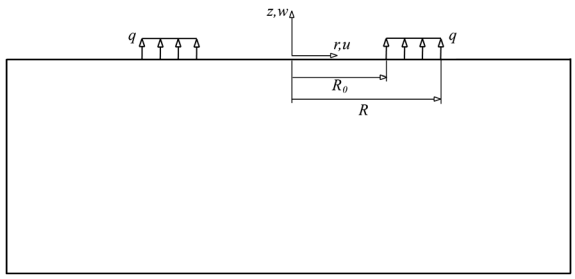

Fig. 10 Uniform tensile load q applied within an annular region $R_0 \le r \le R$ over the surface of the half space. The radial displacement u of the points of this surface is measured along the r-direction, and the vertical displacement w along the z-direction.

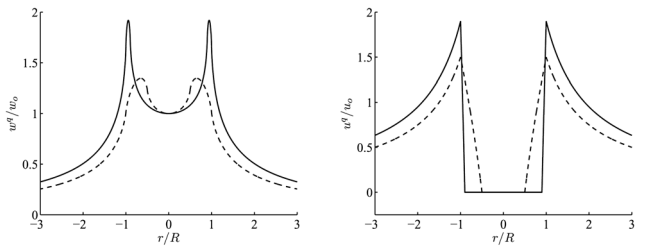

Fig. 11 (a) The vertical displacement w^q along the surface of the substrate due to distributed loading shown in Fig. 10. The normalizing displacement factor is $w_0 = (1 - \nu)q(R - R_0)/G$. The solid curve is for $R_0 = 0.9R$, and the dotted curve for $R_0 = 0.5R$. (b) The corresponding radial displacement u^q. The normalizing displacement factor is $u_0 = (1 - 2\nu)q(R - R_0)/(4G)$.

where

$$W^q = \begin{cases} E\left(\dfrac{r}{R}\right) - \dfrac{R_0}{R}E\left(\dfrac{r}{R_0}\right), & r \le R_0, \\ E\left(\dfrac{r}{R}\right) - \dfrac{r}{R}\left[E\left(\dfrac{R_0}{r}\right) - \left(1 - \dfrac{{R_0}^2}{r^2}\right)K\left(\dfrac{R_0}{r}\right)\right], & R_0 \le r \le R, \\ \dfrac{r}{R}\left[E\left(\dfrac{R}{r}\right) - E\left(\dfrac{R_0}{r}\right) + \left(1 - \dfrac{{R_0}^2}{r^2}\right)K\left(\dfrac{R_0}{r}\right) - \left(1 - \dfrac{R^2}{r^2}\right)K\left(\dfrac{R}{r}\right)\right], & r \ge R. \end{cases}$$

The corresponding radial displacement is obtained in the same way by using eqn (39), with the result

$$u^q = \frac{(1-2\nu)q}{4G}\begin{cases} 0, & r \le R_0, \\ r - \dfrac{{R_0}^2}{r}, & R_0 \le r \le R, \\ \dfrac{R^2 - {R_0}^2}{r}, & r \ge R. \end{cases} \qquad (42)$$

Both eqn (41) and eqn (42) are novel displacement expressions, not reported previously in the literature.

Fig. 11a shows the vertical displacement profile $w^q = w^q(r)$ in the case when $R_0 = 0.9R$ and $0.5R$. The normalizing factor is $w_0 = w^q(0)$. The formation of a blunted ridge under the load with an increase of the interface thickness $R - R_0$ is clear. Fig. 11b shows the corresponding radial displacement $u^q = u^q(r)$. The radial displacement gradient is discontinuous at $r = R_0$ and $r = R$. There is a sharp displacement gradient du/dr between $r = R_0$ and $r = R$, which is sharper for smaller values of the difference $(R - R_0)$, giving rise to displacement discontinuity amounting to $Y(1 - 2\nu)/(2G)$ in the limit $R \to R_0$ and $q(R - R_0) \to Y$, as shown earlier in Fig. 9b. It is noted that $w^q(0) = w^Y(0)$, regardless of the ratio R_0/R.

Fig. 12 shows the total displacement components ($w = w^p + w^q$ and $u = u^p + u^q$), due to the tensile loading q within the range $R_0 \le r \le R$, and the pressure p within $0 \le r < R_0$, in the case of $R_0 = 0.9R$ (w^p and u^p are determined from eqn (29) and eqn (39), in which R_0 plays the role of R). The combined (p, q) loading is self-equilibrating, so that $p = q(R^2 - {R_0}^2)/{R_0}^2$. The load q is

 This journal is © The Royal Society of Chemistry 2012

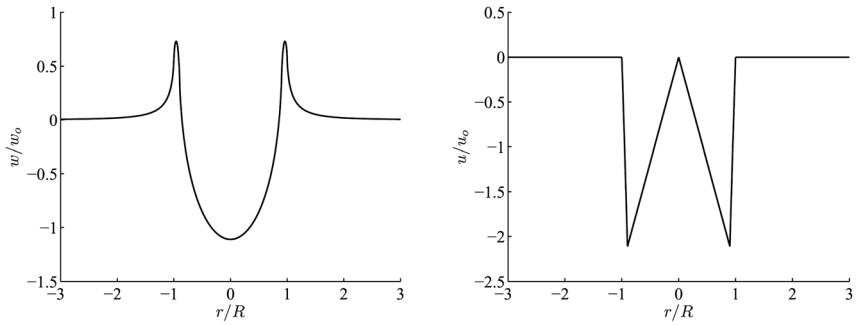

(a) (b)

Fig. 12 (a) The vertical displacement $w = w(r)$ along the surface of the substrate due to tensile loading q shown in Fig. 10 and the pressure $p = q(R^2 - R_0^2)/R_0^2$ within $r < R_0$, where $R_0 = 0.9R$. The normalizing displacement factor is $w_0 = (1 - \nu)p(R - R_0)/G$. (b) The same for the radial displacement. The normalizing displacement is $u_0 = (1 - 2\nu)p(R - R_0)/(4G)$.

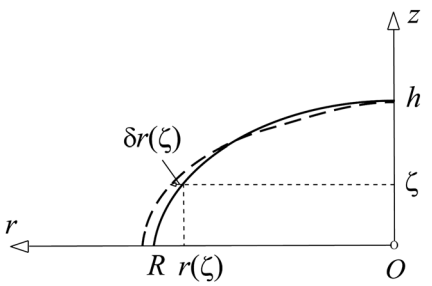

Fig. 13 The virtual displacement $\delta r(\zeta)$ imposed in the r-direction takes the surface of the drop $r = r(\zeta)$ from its solid- to dashed-line configuration. Due to symmetry around the z-axis, only one-half of the surface profile is shown.

statically equivalent to the line tension $Y = \sigma_{sl}\sin\theta$ in the sense that $Y = q(R - R_0)$. Since (p, q) is self-equilibrating, the displacement w diminishes to zero at large r much faster than w^q (*cf.* Fig. 11a and 12a). The vertical displacement at the center is

$$w(0) = -w_0\frac{R}{R_0} = -\frac{(1-\nu)\sigma}{G}\frac{R\sin\theta}{R_0}. \tag{43}$$

Furthermore, since the line force Y is distributed over the finite thickness $R - R_0 = 0.1R$, the discontinuity in the radial displacement at $r = R$ from Fig. 7b is eliminated, albeit the displacement gradient $\mathrm{d}u/\mathrm{d}r$ is still large in the range $0.9R < r < R$ (Fig. 12). The radial displacement vanishes for $r \geq R$ and, by symmetry, at $r = 0$. The remarkable feature of vanishing radial displacement beyond the radius $r = R$ has not been observed in the literature before. Rusanov[12] studied the deformation of an elastic substrate caused by a deposited liquid drop, but did not impose the self-equilibrating nature of the liquid pressure exerted by the drop and the vertical component of adhesive force along the triple-contact line. Furthermore, his analysis did not proceed sufficiently far to reveal the vanishing radial displacement along the substrate outside its contact with the drop. The wetting angle, as determined by Young's equation, is locally not affected by the formation of the blunted ridge due to substrate deformation, as noted in ref. 62.

7. Conclusion

We have presented in this paper a new derivation of both the Young–Laplace equation for the shape of a liquid drop deposited on a solid substrate, and the Young equation for the contact angle between the two. This is accomplished by applying an integral, rather than a local form of the equilibrium condition for an appropriately selected finite portion of the drop, or the entire drop. It is demonstrated that, in the absence of line tension along a triple contact line, neither the contact angle nor the vertical adhesive force exerted on a drop by the substrate, or *vice versa*, depends on the gravity or specific weight of the drop. The simple analysis presented in this paper delivers all mechanics results related to the equilibrium drop's shape and, as such, it represents a valuable complement to the existing variational analysis. The uplifting of the surface of the substrate caused by the vertical adhesive force is determined by using a linear elasticity theory. The singularity in the vertical component and the discontinuity in the radial component of the displacement below the triple contact line are eliminated by distributing the capillary force over a small but finite width around the contact line. It is shown that the radial displacement vanishes on the surface of the substrate outside its contact with a deposited drop. A nonlinear continuum mechanics or an atomistic/molecular dynamics approach is needed to predict the uplifting of the substrate very close to the triple contact line. This is of importance for soft substrates because the formation of circular ridges by the action of capillary forces can have adverse effects on the functioning of MEMS, NEMS, microfluidic and medical devices.

Appendix: variational analysis of a drop's shape and contact angle

We present in this appendix the derivation of Young–Laplace's and Young's equations based on the variational approach and energy minimization. The derivation is closely related to the original derivations from ref. 30 and 31. Under constant ambient pressure and temperature, the free energy of the system, consisting of a liquid drop deposited in the vapor environment on a stiff solid substrate, whose infinitesimal deformation can be ignored, is

$$U = \sigma_{lv}S + (\sigma_{sl} - \sigma_{sv})R^2\pi + 2\pi R\tau + \int_0^h \Delta\gamma z\,\mathrm{d}V. \tag{A1}$$

The last term on the right-hand side of eqn (A1) represents the gravitational potential energy, while

$$S = \int_0^h 2\pi r(z)\mathrm{d}s, \quad \mathrm{d}s = \left[1 + r'^2(z)\right]^{1/2}\mathrm{d}z \tag{A2}$$

is the surface of the axisymmetric liquid–vapor interface, whose profile $r = r(z)$ is to be determined. If the liquid is assumed to be incompressible and if there is no evaporation, the liquid volume V remains constant and the appropriate functional for the variational study is

$$\Pi = U - \lambda V, \quad V = \int_0^h r^2(z)\pi\mathrm{d}z. \tag{A3}$$

The Lagrangian multiplier λ has the dimension of pressure. In view of eqn (A1) and eqn (A2), the potential function Π can be written as

$$\Pi = \int_0^h \Phi(z, r, r')\mathrm{d}z, \tag{A4}$$

where

$$\Phi = \sigma_{\mathrm{lv}} 2\pi r(z)\left[1 + r'^2(z)\right]^{1/2} - r^2(z)\pi(\lambda - z\Delta\gamma) + \frac{1}{h}\left[(\sigma_{\mathrm{sl}} - \sigma_{\mathrm{sv}})r^2(z)\pi + 2\pi r(z)\tau\right]\bar{\delta}(z). \tag{A5}$$

The Dirac delta function is $\bar{\delta}(z)$, and h is the height of the drop. The variation of the functional $\delta\Pi$, divided by an infinitesimal variation $\delta r(\zeta)$ at an arbitrary $z = \zeta$ (Fig. 13), must vanish at the equilibrium state,

$$\frac{\delta\Pi}{\delta r(\zeta)} = h\left[\frac{\partial\Phi}{\partial r} - \frac{\mathrm{d}}{\mathrm{d}z}\left(\frac{\partial\Phi}{\partial r'}\right)\right]_{z=\zeta} + \left[\frac{\partial\Phi}{\partial r'}\bar{\delta}(z - \zeta)\right]_{z=0}^{z=h} = 0. \tag{A6}$$

The first term on the right-hand side yields the Euler–Lagrange's differential equation, while the second term accounts for the boundary conditions. From eqn (A5), it readily follows that

$$\begin{aligned}
\frac{\partial\Phi}{\partial r} &= 2\pi\left[\sigma_{\mathrm{lv}}(1 + r'^2)^{1/2} - r(\lambda - z\Delta\gamma)\right] + \frac{2\pi}{h}\left[R(\sigma_{\mathrm{sl}} - \sigma_{\mathrm{sv}}) + \tau\right]\bar{\delta}(z),\\
\frac{\partial\Phi}{\partial r'} &= 2\pi\sigma_{\mathrm{lv}}\frac{rr'}{(1 + r'^2)^{1/2}},\\
\frac{\mathrm{d}}{\mathrm{d}z}\left(\frac{\partial\Phi}{\partial r'}\right) &= 2\pi\sigma_{\mathrm{lv}}\left[(1 + r'^2)^{1/2} - 2r\kappa\right].
\end{aligned} \tag{A7}$$

The mean curvature of the drop's profile is the arithmetic mean of the two principal curvatures,

$$\kappa = \frac{1}{2}(\kappa_1 + \kappa_2), \quad \kappa_1 = \frac{1}{r(1 + r'^2)^{1/2}}, \quad \kappa_2 = -\frac{r''}{(1 + r'^2)^{3/2}}. \tag{A8}$$

Furthermore, in view of the second expression in eqn (A7),

$$\left[\frac{\partial\Phi}{\partial r'}\bar{\delta}(z - \zeta)\right]_{z=0}^{z=h} = 2\pi R\sigma_{\mathrm{lv}}\cos\theta\bar{\delta}(\zeta), \tag{A9}$$

because the slope at the apex of the drop $r'(h)$ vanishes by symmetry, and the cosine of the angle between the tangent to the drop's profile and the horizontal surface of the substrate is

$$\cos\theta = -\frac{r'(0)}{\left[1 + r'^2(0)\right]^{1/2}}. \tag{A10}$$

Consequently, by substituting eqn (A7) and eqn (A9) into eqn (A6), there follows

$$2\pi hr(\zeta)\left[2\sigma_{\mathrm{lv}}\kappa(\zeta) - \lambda + \zeta\Delta\gamma\right] + 2\pi R\left(\sigma_{\mathrm{lv}}\cos\theta + \sigma_{\mathrm{sl}} - \sigma_{\mathrm{sv}} + \frac{\tau}{R}\right)\bar{\delta}(\zeta) = 0. \tag{A11}$$

For this to vanish, the two terms must vanish separately, which gives

$$\lambda - 2\sigma_{\mathrm{lv}}\kappa(\zeta) - \zeta\Delta\gamma = 0, \tag{A12}$$

and

$$\sigma_{\mathrm{sv}} - \sigma_{\mathrm{sl}} - \sigma_{\mathrm{lv}}\cos\theta - \frac{\tau}{R} = 0. \tag{A13}$$

The last expression is a modified Young's equation, incorporating the line tension τ.[44,45] Eqn (A12) yields the differential equation for the shape of the drop. To determine an expression for the Lagrangian multiplier λ, the fact that the surface of the drop near the apex $z = h$ is locally a sphere, of some radius b, so that eqn (A12) gives $\lambda = h\Delta\gamma + 2\sigma_{\mathrm{lv}}/b$ is used. Since $\Delta p(h) = 2\sigma_{\mathrm{lv}}/b$, by the elementary consideration of a pressurized spherical shell, the Lagrangian multiplier can also be interpreted as the pressure difference between the liquid and vapor phases at $z = 0$, *i.e.*, $\lambda = \Delta p(0) = \Delta p(h) + h\Delta\gamma$. Thus, eqn (A12) can be rewritten in the form of Young–Laplace's equation $2\sigma_{\mathrm{lv}}\kappa(\zeta) = \Delta p(\zeta)$, where $\Delta p(\zeta) = \Delta p(0) - \zeta\Delta\gamma$.

Acknowledgements

This research was supported by the Montenegrin Academy of Sciences and Arts. Valuable discussions with professors Prabhakar Bandaru and Frank E. Talke are also acknowledged.

References

1 W. A. Zisman, Relation of the equilibrium contact angle to liquid and solid constitution, in *Contact Angle, Wettability, and Adhesion*, ed. R. F. Gould, American Chemical Society, Washington, D. C., 1964, pp. 1–51.
2 P. G. de Gennes, F. Brochard-Wyart and D. Quéré, *Capillarity and Wetting Phenomena*, Springer, Berlin, 2004.
3 C. A. Miller and P. Neogi, *Interfacial Phenomena. Equilibrium and Dynamic Effects*, CRC Press, Boca Raton, FL, 2nd edn, 2008.
4 T. Young, An essay on the cohesion of fluids, *Philos. Trans. R. Soc. London*, 1805, **95**, 65–87.
5 P. S. Laplace, *Theory of Capillary Attraction. Supplement of Celestial Mechanics*, 1805, p. 394.
6 P. G. de Gennes, Wetting: statics and dynamics, *Rev. Mod. Phys.*, 1985, **57**, 827–863.
7 R. Finn, The contact angle in capillarity, *Phys. Fluids*, 2006, **18**, 047102.
8 R. Finn, Comments related to my paper. The contact angle in capillarity, *Phys. Fluids*, 2008, **20**, 107104.
9 I. Lunati, Young's law and the effects of interfacial energy on the pressure at the solid–liquid interface, *Phys. Fluids*, 2007, **19**, 118105.

 This journal is © The Royal Society of Chemistry 2012

10 D. Shikhmurzaev, On Youngs (1805) equation and Finns (2006) counterexample, *Phys. Lett. A*, 2008, **372**, 704–707.
11 G. R. Lester, Contact angles of liquids at deformable solid surfaces, *J. Colloid Sci.*, 1961, **16**, 315–326.
12 A. I. Rusanov, Theory of the wetting of elastically deformed bodies. 1. Deformation with a finite contact angle, *Colloid J. USSR*, 1975, **37**, 614–622.
13 M. A. Fortes, Deformation of solid-surfaces due to capillary forces, *J. Colloid Interface Sci.*, 1984, **100**, 17–26.
14 M. E. R. Shanahan, The spreading dynamics of a liquid-drop on a viscoelastic solid, *J. Phys. D: Appl. Phys.*, 1988, **21**, 981–985.
15 R. Kern and P. Muller, Deformation of an elastic thin solid induced by a liquid droplet, *Surf. Sci.*, 1992, **264**, 467–494.
16 A. Carré, J.-C. Gastel and M. E. R. Shanahan, Viscoelastic effects in spreading of liquids, *Nature*, 1996, **379**, 432–434.
17 L. R. White, The contact angle on an elastic substrate. 1. The role of dis-joining pressure in the surface mechanics, *J. Colloid Interface Sci.*, 2003, **258**, 82–96.
18 R. Pericet-Camára, A. Best, H.-J. Butt and E. Bonaccurso, Effect of capillary pressure and surface tension on the deformation of elastic surfaces by sessile liquid microdrops: an experimental investigation, *Langmuir*, 2008, **24**, 10565–10568.
19 R. Pericet-Camára, G. K. Auernhammer, K. Koynov, S. Lorenzoni, R. Raiteri and E. Bonaccurso, Solid-supported thin elastomer films deformed by microdrops, *Soft Matter*, 2009, **5**, 3611–3617.
20 Y.-S. Yu and Y.-P. Zhao, Elastic deformation of soft membrane with finite thickness induced by a sessile liquid droplet, *J. Colloid Interface Sci.*, 2009, **339**, 489–494.
21 J. L. Liu, Z. X. Nie and W. G. Jiang, Deformation field of the soft substrate induced by capillary force, *Phys. B*, 2009, **404**, 1195–1199.
22 B. Roman and J. Bico, Elasto-capillarity: deforming an elastic structure with a liquid droplet, *J. Phys.: Condens. Matter*, 2010, **22**, 493101.
23 E. R. Jerison, Y. Xu, L. A. Wilen and E. R. Dufresne, Deformation of an elastic substrate by a three-phase contact line, *Phys. Rev. Lett.*, 2011, **106**, 186103.
24 S. Das, A. Marchand, B. Andreotti and J. H. Snoeijer, Elastic deformation due to tangential capillary forces, *Phys. Fluids*, 2011, **23**, 072006.
25 D. A. Porter and K. E. Easterling, *Phase Transformations in Metals and Alloys*, CRC, Taylor & Francis Group, Boca Raton, FL, 2004.
26 J. S. Rowlinson and B. Widom, *Molecular Theory of Capillarity*, Clarendon, Oxford, 1982.
27 F. Neumann, *Vorlesungen über die Theorie der Capillarität*, B.G. Teubner, Leipsig, Germany, 1984.
28 F. G. Yost, Fundamentals of Wetting and Spreading with Emphasis on Soldering, in *The Metal Science of Joining*, ed. M. J. Cieslak, *et al.*, The Minerals, Metal, and Materials Society, Warrendale, PA, 1992, pp. 49–74.
29 J. W. Gibbs, *Collected Works*, Dover, New York, 1961.
30 R. E. Johnson, Conflicts between Gibbsian thermodynamics and recent treatments of interfacial energies in solid–liquid–vapor, *J. Phys. Chem.*, 1959, **63**, 1655–1658.
31 E. M. Blokhuis, Y. Shilkrot and B. Widom, Young's law with gravity, *Mol. Phys.*, 1995, **86**, 891–899.
32 G. Whyman, E. Bormashenko and T. Stein, The rigorous derivation of Young, Cassie-Baxter and Wenzel equations and the analysis of the contact angle hysteresis phenomenon, *Chem. Phys. Lett.*, 2008, **450**, 355–359.
33 E. M. Blokhuis, Liquid Drops at Surfaces, in *Surface and Interfacial Tension: Measurement, Theory, and Applications, Surfactant Science Series, Vol. 119*, ed. S. Hartland, Marcel Dekker, Inc., New York, 2005, pp. 147–193.
34 E. Bormashenko, Young, Boruvka-Neumann, Wenzel and Cassie–Baxter equations as the transversality conditions for the variational problem of wetting, *Colloids Surf., A*, 2009, **345**, 163–165.
35 V. A. Lubarda and K. A. Talke, Configurational forces and shape of a sessile droplet on a rotating solid substrate, *Theor. Appl. Mech.*, 2012, **39/1**, 27–54.
36 J. J. Bikerman, Contact Angles, Spreading and Wetting, in *Electrical Phenomena. Solid/Liquid Interface (Proceedings of the Second Int. Congress of Surface Activity), Vol. III*, ed. J.H. Schulman, Academic Press, New York, 1957, pp. 125–130.
37 B. A. Pethica, The contact angle equilibrium, *J. Colloid Interface Sci.*, 1977, **62**, 567–569.
38 H. Fujii and H. Nakae, Effects of gravity on contact angle, *Philos. Mag. A*, 1995, **72**, 1505–1512.
39 Y. Liu and R. M. German, Contact angle and solid–liquid–vapor equilibrium, *Acta Mater.*, 1996, **44**, 1657–1663.
40 Y. Larher, A very simple derivation of Young's law with gravity using a cylindrical meniscus, *Langmuir*, 1997, **13**, 7299–7300.
41 E. Bormashenko and G. Whyman, Variational approach to wetting problems: calculation of a shape of sessile liquid drop deposited on a solid substrate in external field, *Chem. Phys. Lett.*, 2008, **463**, 103–105.
42 R. D. Cook and W. C. Young, *Advanced Mechanics of Materials*, Prentice Hall, Upper Saddle River, New Jersey, 2nd edn, 1999.
43 A. C. Ugural and S. K. Fenster, *Advanced Mechanics of Materials and Applied Elasticity*, Prentice Hall, Upper Saddle River, New Jersey, 5th edn, 2012.
44 L. Boruvka and A. W. Neumann, Generalization of the classical theory of capillarity, *J. Chem. Phys.*, 1977, **66**, 5464–5476.
45 B. Widom, Line tension and the shape of a sessile drop, *J. Phys. Chem.*, 1995, **99**, 2803–2806.
46 T. Pompe and S. Herminghaus, Three-phase contact line energetics from nanoscale liquid surface topographies, *Phys. Rev. Lett.*, 2000, **85**, 1930–1933.
47 A. D. Dussaud and M. Vignes-Adler, Line Tension Effect on Alkane Droplets Near Wetting Transition, in *Dynamics of Small Confining Systems III. MRS Proceedings, Vol. 464*, ed. J. M. Drake, J. Klafter, and R. Kopelman, Materials Research Society, Pittsburgh, PA, 1997, pp. 287–293.
48 P. Blecua, R. Lipowsky and J. Kierfeld, Line tension effects for liquid droplets on circular surface domains, *Langmuir*, 2006, **22**, 11041–11059.
49 J. K. Berg, C. M. Weber and H. Riegler, Impact of negative line tension on the shape of nanometer-size sessile droplets, *Phys. Rev. Lett.*, 2010, **105**, 076103.
50 A. E. H. Love, The stress produced in a semi-infinite solid by pressure on part of the boundary, *Philos. Trans. R. Soc. London, Ser. A*, 1929, **228**, 377–420.
51 S. P. Timoshenko and J. N. Goodier, *Theory of Elasticity*, McGraw-Hill, New York, 3rd edn, 1970.
52 K. L. Johnson, *Contact Mechanics*, Cambridge University Press, New York, 1985.
53 I. S. Gradshteyn and I. W. Ruzhik, *Tables of Integrals, Sums and Products*, Academic Press, New York, 1965.
54 V. A. Lubarda and K. A. Talke, An analysis of the equilibrium droplet shape based on an ellipsoidal droplet model, *Langmuir*, 2011, **27**, 10705–10713.
55 M. E. R. Shanahan, The influence of solid micro-deformation on contact angle equilibrium, *J. Phys. D: Appl. Phys.*, 1987, **20**, 945–950.
56 J. Olives, Capillarity and elasticity the example of the thin plate, *J. Phys.: Condens. Matter*, 1993, **5**, 2081–2094.
57 J. Olives, A combined capillarity and elasticity problem for a thin plate, *SIAM J. Appl. Math.*, 1996, **56**, 480–493.
58 J. Olives, Surface thermodynamics, surface stress, equations at surfaces and triple lines for deformable bodies, *J. Phys.: Condens. Matter*, 2010, **22**, 085005.
59 R. Tadmor, Approaches in wetting phenomena, *Soft Matter*, 2011, **7**, 1577–1580.
60 M. E. R. Shanahan and P. G. de Gennes, Equilibrium of the triple line solid/liquid/fluid of a sessile drop, in *Adhesion 11*, ed. K. W. Allen, Elsevier Appl. Sci., London, 1987, ch. 5, pp. 71–81.
61 V. A. Lubarda, Circular loads on the surface of a half-space: displacement and stress discontinuities under the load, *Int. J. Solids Struct.*, 2012, accepted.
62 D. J. Srilovitz and S. H. Davis, Do stresses modify wetting angles, *Acta Mater.*, 2001, **49**, 1005–1007.